J Solid State Electrochem (2010) 14:523–530
DOI 10.1007/s10008-008-0684-2

ORIGINAL PAPER

Influence of the electropolymerisation mode on PEDOTh films morphology and redox behaviour—an AFM investigation

A. I. Melato · A. S. Viana · L. M. Abrantes

Received: 18 July 2008 / Revised: 18 September 2008 / Accepted: 18 September 2008 / Published online: 15 October 2008

Abstract The morphologies of PEDOTh films deposited on platinum electrodes, using different electrochemical modes but conditions selected to obtain layers with similar electroactivities, have been analysed by atomic force microscopy (AFM). *Ex situ* AFM showed a fibber-like topography for the potentiodynamically synthesised films, contrasting to the granular character of those formed at constant potential. *In situ* contact mode AFM, used to examine the initial stages of the polymer growth and the surface morphology evolution, disclosed the development of long segments with the number of potential cycles, and the formation of identical globular nodules, which diameter increases with the growth charge. The morphological changes imparted by the switching process revealed to be more marked in films grown at constant potential. Thickness measurements performed on oxidised and reduced films unveiled the swelling/shrinking of the polymers during the ingress/egress of the perchlorate anions, with film volume changes of ca. 20% upon oxidation.

Keywords Poly(3,4-ethylenedioxythiophene) · Atomic force microscopy · Redox behaviour · Polymer swelling/shrinking

Contribution to the Fifth Baltic Conference on Electrochemistry, 30 April - 3 May 2008, Tartu, Estonia.

A. I. Melato · A. S. Viana · L. M. Abrantes (✉)
CQB, Departamento de Química e Bioquímica,
Faculdade de Ciências da Universidade de Lisboa,
Campo Grande 1749-016 Lisboa, Portugal
e-mail: luisa.abrantes@fc.ul.pt

Introduction

During the last years, studies devoted to the electropolymerisation and to the influence of the electrochemical mode and conditions on the properties of the obtained conducting polymers have successfully used scanning probe microscopy (SPM).

With regard to the film formation, Chao et al. [1, 2] have used *ex situ* atomic force microscopy, AFM, to characterize the morphology of poly(3-methylthiophene) films in different stages of the potentiostatic deposition. The authors observed the nucleation and formation of different polymer layers on the electrode surface, with distinct characteristics. Suárez and Compton [3] proved that the morphology of a polypyrrole film in the initial steps of deposition depends on the electrode material showing that a more homogeneous growth is visible upon glassy carbon and gold than over platinum. Other authors [4] report the strong influence of ITO substrate on the morphology of a polyaniline film during the early stages of the electropolymerization. The galvanostatic deposition of polybithiophene was also investigated by *in situ* AFM [5].

Aiming to correlate the electropolymerisation experimental parameters and the attributes of the polymer, Bard et al. [6] using scanning tunnelling microscopy, STM, showed that the morphology of polyaniline depends on the potential scan rate applied during the polymer synthesis. As demonstrated by Mourato et al. [7] through AFM, heterogeneous and porous polyaniline films are obtained at 60 mV s^{-1}, while at 10 mV $s^{-1,}$ a more compact layer is formed. More recently, other experimental issues, such as the electrochemical mode (potentiostatic or potentiodynamic) [8], the supporting electrolyte nature [8–10], and the monomer concentration [11] have also been addressed in studies by AFM.

Poly(3,4-ethylenedioxythiophene) (PEDOTh) and derivatives have been extensively investigated due to their well-known properties (e.g. high conductivity, low oxidation potential, and excellent stability in the oxidised state). Among these studies very relevant information, delivered by SEM, *ex situ* AFM (including current sensing AFM [12]) or STM [13], has been obtained on the influence of several electrosynthesis parameters (such as electropolymerisation method [14, 15], pH [14], substrate [13], film thickness/deposition time [16], potential and current limits [15]) on the films morphology, local electrical properties or even on potentiometric performance towards compounds of biological importance [16]. It was demonstrated that in similarity with the observed for other conducting polymers, one can tune the final films morphology (e.g. globular, "nano-fungus like," fibrillar, etc.) using the appropriate electrodeposition conditions. However, to the best of our knowledge, there is no report in the literature on *in situ* AFM investigations following PEDOTh electrodeposition process, where it is shown in real-time the effect of a given electropolymerisation condition on the initial stages of polymer formation. This is in high contrast with the large number of publications for other conducting polymers, such as polybithiophene, polymethylthiophene, polyaniline, or polypyrrole, where surface modifications during electropolymerisation and also induced by the redox behaviour of the polymer films are thoroughly studied, as mentioned above.

In a previous recent study, devoted to a detailed analysis of the potentiostatic deposition of PEDOTh, the authors reported [17] the initial formation of a compact film followed by a more porous and less ordered one; thus when relatively high growth charges are employed, at least a two-layered polymer must be expected. Differences in the redox behaviour of thin and tick PEDOTh layers, namely, an easier de-doping of the top layer, and the corresponding features observed for PEDOTh prepared under multiple potential cycling, guided our interest in a further investigation on the evolution of the polymer morphology with the number of potential cycles, here reported.

In the present study, the influence of the deposition method, potentiostatic or potentiodynamic, on the morphology of PEDOTh films with similar electroactivity is discussed. The evolution of the polymer topography with the number of polymerisation cycles or with the deposition charge, is monitored in real-time using *in situ* contact mode AFM. The morphological features of the obtained films are compared with the ones electrosynthesised in a conventional cell and imaged in ambient conditions, using tapping mode AFM. The redox behaviour of the PEDOTh films, grown by the two distinct electrochemical routes, is also examined by following the topographical modifications and the changes in the film thickness occurring when the polymer is switched from the oxidised to the reduced forms.

Experimental

The monomer 3,4-ethylenedioxythiophene, EDOTh (Aldrich) was distilled under reduced pressure prior to use. The solvent, acetonitrile, ACN (HPLC grade, Aldrich 99.93%), was previously dried in calcium hydride and distilled with phosphorus pentoxide under N_2 atmosphere. The supporting electrolyte, tetrabutylammonium perchlorate, $TBAClO_4$ (Fluka, puriss. ≥ 99%) was previous recrystallised from ethanol. Prior to the measurements, the solutions were deaerated by bubbling N_2 (high purity, dried) for 20 min.

Two different working electrodes were used; a platinum disk (A=0.196 cm^2) sealed with epoxy resin into a Teflon holder and thin layer Pt (200 nm) slides evaporated onto borosilicate glass (Arrandee™, GmbH). In the case of the platinum disks, for each experiment, a fresh mirror-finish surface was generated by hand-polishing the electrode in an aqueous suspension of successively finer grades of alumina (down to 0.05 μm). Thin layer Pt electrodes were cleaned in hot piranha solution followed by potential cycling in 0.25 mol dm^{-3} H_2SO_4. A Pt foil and a saturated calomel electrode (SCE) were used as counter and reference electrode, respectively.

The PEDOTh electropolymerisation was performed under potentiodynamic and potentiostatic modes using a 0.02 M EDOTh in 0.1 M $TBAClO_4$ acetonitrile solution. PEDOTh films were potentiodynamically grown by cycling the potential between −0.8 and +1.18 V for the first five cycles, then lowering the anodic limit to 1.16 V for the next three cycles, and to 1.15 V for the following cycles, at 50 mV s^{-1} sweep rate (ν). The potentiostatic deposition was carried out at 1.20 V (E_g) as described elsewhere [14].

The films were electrochemically characterized, using a two-compartment cell, in a 0.1 M $TBAClO_4$ monomer free solution by cycling the potential between −1.20 and 1.20 V, at ν=50 mV s^{-1}.

The electrochemical experiments were carried out on a CH Instruments electrochemical analyser, model 600A, controlled by a personal computer, using a conventional three-electrode and two-compartment cell. AFM images were collected in a MultiMode atomic force microscope running on the NanoScope IIIa controller (Digital Instrument, Veeco). A commercial electrochemical AFM (ECAFM) cell (Digital Instruments, Veeco) containing platinum wires as counter and pseudo-reference electrodes was used. The platinum wires were flame-annealed before each experiment. The stability of the pseudo-reference electrode in the ECAFM cell was routinely checked, and the voltammograms obtained were compared to the ones recorded in a conventional electrochemical cell with a saturated calomel electrode. Therefore, all potentials cited in this paper have been converted to SCE.

The *ex situ* AFM images were obtained in tapping mode, using etched silicon tips (resonance frequency of ca. 300 kHz), whereas the *in situ* measurements were performed in contact mode, using V-shape silicon nitrite cantilevers.

Results and discussion

It is known that PEDOTh, like many other electronically conducting polymers, can be prepared under different electrochemical modes [18–21]. Figure 1 illustrates that under particular conditions, namely, potentiostatic growth at E_g=1.20 V vs. SCE, with a deposition charge of 30 mC cm^{-2} and potentiodynamic electropolymerisation at 50 mV s^{-1}, [−0.8, +1.18] V vs. SCE for 30 cycles, PEDOTh layers displaying similar electroactivity can be attained.

The voltammetric redox conversion characteristics of the so-obtained PEDOTh films are summarized in Table 1. There is a slight shift in the redox peaks potential (more positive for the potentiodynamically grown polymer) but the most noteworthy difference is the magnitude of the cathodic peak R2, more intense than R1 for the film prepared under constant potential. An increase of the R1 peak intensity with polymer thickening has been previously observed [17] and attributed to an easier egress of counter-ions from a less dense outer layer, deposited on the top of a first compact thin film accountable for R2. In analogy, the higher peaks intensity ratio, R1/R2, perceived for PEDOTh formed under multiple potential cycles, strongly suggests that this synthetic route generates more porous layers.

As shown in Fig. 2, the AFM characterisation of the films reveals a fibber-like morphology for the potentiodynamically prepared polymer contrasting to the granular aspect of the potentiostatically formed one. In addition, the surface roughness observed for the first one, as confirmed by the root mean square roughness value (denoted as R_q), is almost double of the obtained for the layer grown under potentiostatic mode, i.e., 100 and 55 nm, respectively. Thus, the ingress and expulsion of counter-ions (ClO_4^-) that occurs during each polymerisation cycle shall promote the formation of longer polymer segments and subsequent branches instead of cauliflower-like arrangement seen for PEDOTh deposited under constant potential.

To get a deeper insight on the effect of the electrosynthetic mode on the morphology of PEDOTh layers, the polymer formation by both approaches has been followed by *in situ* AFM. In these studies, it was compulsory to use a flat platinum slide as working electrode and to slightly lower the applied potential for monomer oxidation used in the conventional electrochemical cell, to enable the observation of the polymer deposition, in real time, without too much interference from the scanning tip.

Therefore, the potentiostatic growth of PEDOTh has been carried out at 1.09 V, value at the very beginning of the current onset due to monomer oxidation. An illustrative sequence of AFM images is displayed in Fig. 3. Nucleation is noticed after consumption of 0.24 mC cm^{-2}, as denoted by the white line in Fig. 3a; once 0.63 mC cm^{-2} growth charge is used (bottom of this figure), the nucleus are clearly visible.

As the polymer growth proceeds (5 mC cm^{-2}; Fig. 3b), the platinum surface is covered by grains with approximately 100 nm and few nodules (diameter ~175 nm) can be noticed. The lines in this figure are imaging artefacts produced by the tip interaction with the hitherto formed polymer. Globules of about the same size keep developing

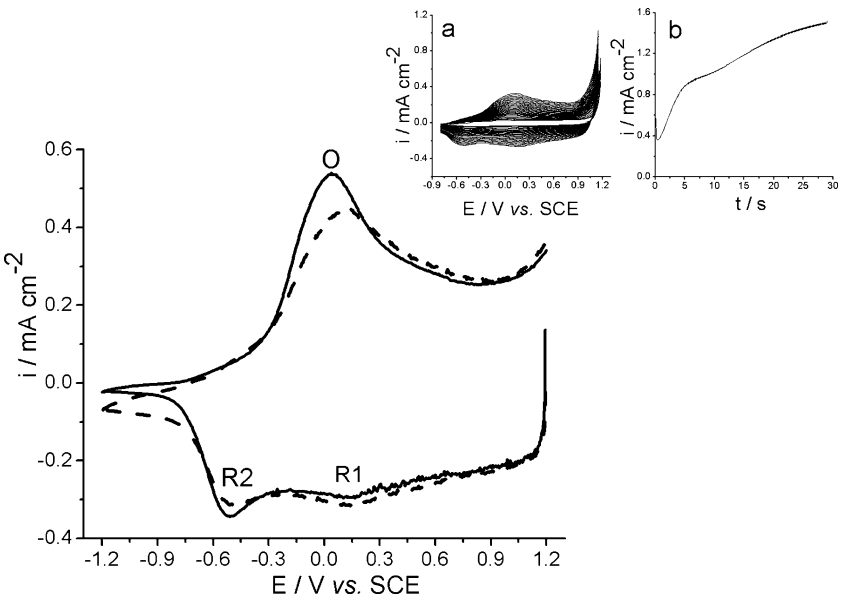

Fig. 1 Cyclic voltammograms of PEDOTh films prepared on Pt under (*broken lines*) potentiodynamic (30 cycles) and (*straight lines*) potentiostatic (E_g=1.20 V) control from 0.02 mol dm^{-3} EDOTh in 0.1 mol dm^{-3} $TBAClO_4$ acetonitrile solution, in monomer free solution, υ=50 mV s^{-1}. Insert: **a** potentiodynamic electropolymerisation of EDOTh at 50 mV s^{-1}, [−0.8, +1.18] V vs. SCE, and **b** current-time transient recorded during the potentiostatic growth of PEDOTh at E_g=1.20 V, up to Q_g=30 mC cm^{-2}

Table 1 Voltammetric characteristics for the redox behaviour of PEDOTh films prepared under potentiodynamic (30 cycles) and potentiostatic control (with Q_g=30 mC cm^{-2})

Growth mode	E_p^O/*V* vs SCE	E_p^{R1}/*V* vs SCE	E_p^{R2}/*V* vs SCE	Q_O/mC cm^{-2}	Q_R/mC cm^{-2}	Q_O/Q_R
Consecutive potential cycling						
50 mV s^{-1}, [−0.8, +1.18] V *vs.* SCE	0.130	0.150	−0.495	10.0	10.4	0.96
Constant potential						
1.20 V; Q_g=30 mC cm^{-2}	0.040	0.130	−0.510	10.5	10.1	1.0

as the deposition time increases (Fig. 3c and d), and a globular morphology can be clearly observed as soon as 11 mC cm^{-2} are consumed (Fig. 3d). As reported by Patra et al., potentiostatically formed PEDOTh films present similar morphologies as revealed by SEM images [15].

In what concerns the *in situ* AFM study of the PEDOTh potentiodynamic growth, Fig. 4 shows the evolution of the film morphology with the number of polymerisation cycles. The surface of polycrystalline Pt (Fig. 4a) is already modified after the first potential cycle as shown by Fig. 4b, and nucleus coalescence appears to occur after two cycles (Fig. 4c); these elongated features develop into fibber-like patterns, clearly visible from the fourth to the tenth cycle (Fig. 4d to f). Unfortunately it was not possible to follow, with an acceptable image quality, thicker films, since very large interactions between the tip and the polymeric matrix were obtained, most probably due to the polymer structural rearrangements occurring during the egress/ingress of counter-ions accompanying the reduction/oxidation of the polymer. Actually, using a low imaging force, it was observed that AFM images were lost after the reduction process and only recovered when the potential reached again the value for polymer oxidation, whereas with higher imaging forces, the image is not lost after polymer reduction. These observations are consistent with the swelling and shrinking of the polymer matrix during its oxidation/reduction processes, due to the ingress/egress of the ClO_4^- anions, as charge compensators. At low force, when the polymer shrinks, the tip cannot reach the surface, and therefore, the image is lost. In contrast, at higher forces upon oxidation and polymer swelling, there is a higher tip–surface interaction which affects the image resolution.

In order to overcome this experimental limitation and aiming to confirm the fibrillar character of the potentiodynamic formed PEDOTh, films with distinct number of polymerisation cycles (from 2 until 30) were electrosynthesised *ex situ* in a conventional three-electrode cell; Fig. 5 illustrates the respective redox behaviour.

The ill-defined redox conversion observed at the modified electrode after carrying out two electropolymerisation cycles is due to an incomplete electrode coverage by the polymer, as supported by the AFM image (Fig. 6a). However, the oxidation and the two reduction waves are detectable in a PEDOTh film prepared with six cycles, in contrast to what is observed for the potentiostatically grown layers [17], where only R2 can be clearly distinguished. A different organisation/configuration towards a less dense and more porous material must be expected, in order to explain the earlier polymer reduction displayed by the thin PEDOTh films synthesised by multiple potential cycling, in comparison to the polymers obtained under constant potential [17, 22]. In fact, 6 potential cycles produce an assembly of small and elongated grains as can be observed in Fig. 6b, where some fibrillar features can be already depicted. Increasing the number of

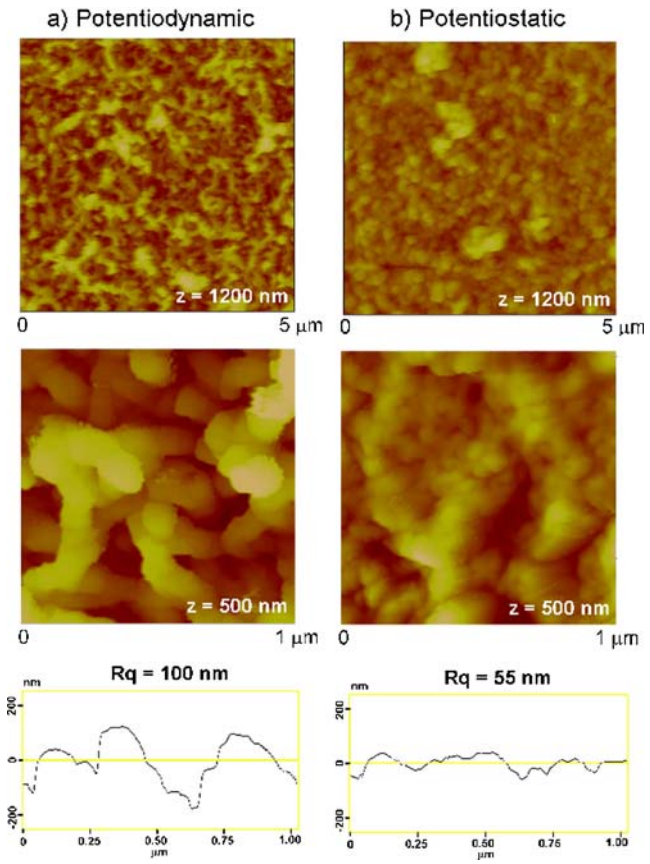

Fig. 2 AFM images of PEDOTh films formed under **a** potentiodynamic and **b** potentiostatic mode; same conditions as Fig. 1

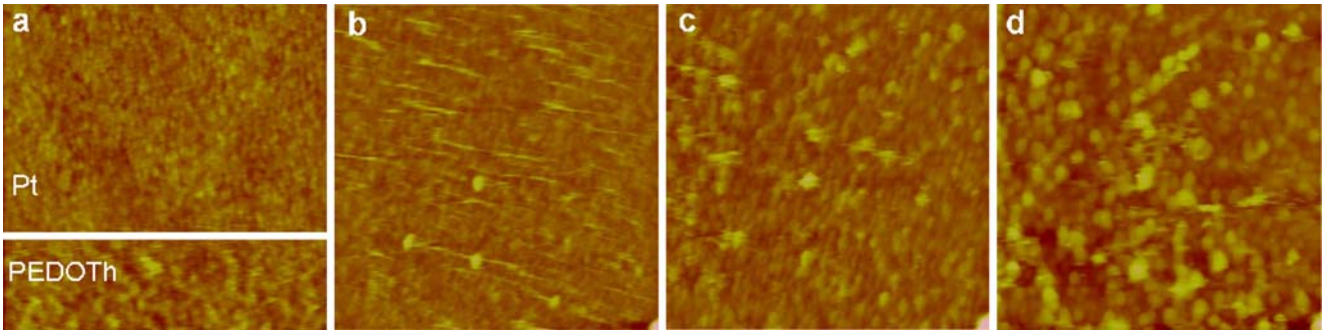

Fig. 3 *In situ* AFM images (5×5 μm^2) of PEDOTh potentiostatic growth at 1.09 V on a Pt slide from 0.02 mol dm^{-3} in 0.1 mol dm^{-3} $TBAClO_4$ acetonitrile solution; **a** Q_g=0.63 mC cm^{-2}, z=10 nm; **b** Q_g=5.3 mC cm^{-2}, z=100 nm; **c** Q_g=9.0, and **d** 11.2 mC cm^{-2}, z=150 nm

cycles, the grains evolute to fibres, well visible after 15 cycles, Fig. 6c, and fibber-like clusters develop as illustrated by Fig. 6d (30 cycles). As expected, the surface roughness value, *Rq*, increases as the electropolymerisation proceeds, being very large (four times), the increment from 15 to 30 cycles, indicating a great augment in the polymer porosity.

The morphological changes associated with the doping and de-doping process of PEDOTh films, due to the ingress/egress of the ions have also been investigated by *in situ* contact mode AFM, as depicted in Fig. 7. For this purpose, two films displaying similar electroactivity ($Q_o \approx$ 4.75 mC cm^{-2}, $Q_o/Q_r \approx 1$), one grown potentiodynamically with 15 cycles (Fig. 7a and b) and the other synthesised potentiostatically at 1.2 V, with a growth charge of 21 mC cm^{-2} (Fig. 7c and d), have been imaged after electrode polarisation, in monomer-free electrolyte solution during 5 min, at −1.0 V (reduced state, Fig. 7a and c) and 1.0 V (oxidized state, Fig. 7b and d).

Although the polymer switching process produces a dramatic morphological change in both films, this variation is more marked for the film grown at constant potential. In this case, PEDOTh displays a more compact morphology (as discussed above for images recorded in air, using *tapping* mode AFM, Fig. 2), and thus the harder ingress/egress of ions during the oxidation/reduction of the film may cause greater polymer matrix rearrangements.

In Fig. 7, it can also be observed that, upon oxidation and independently of the electrosynthesis mode, there is an increase in size of the respective polymer pattern. This event, reversible with potential switching (data not shown), is very likely associated to the widely reported film swelling/shrinking, as outcome of conducting polymer redox conversion [23, 24].

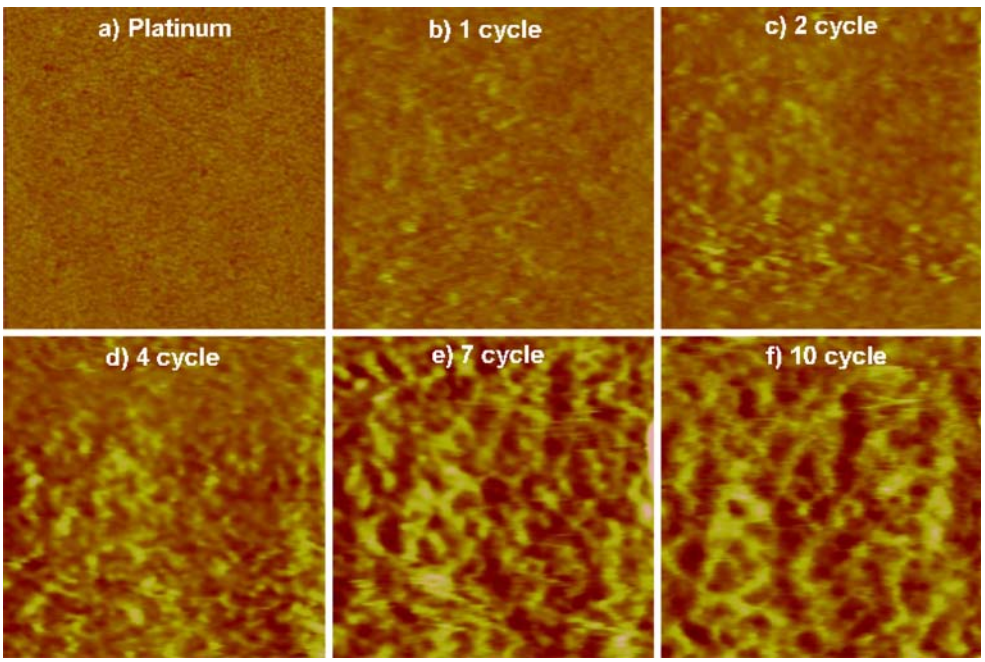

Fig. 4 *In situ* AFM images (2×2 μm^2) of the potentiodynamic growth of a PEDOTh film in Pt slide from 0.02 mol dm^{-3} in 0.1 mol dm^{-3} $TBAClO_4$ acetonitrile solution, υ=50 mV s^{-1}. z=30 nm

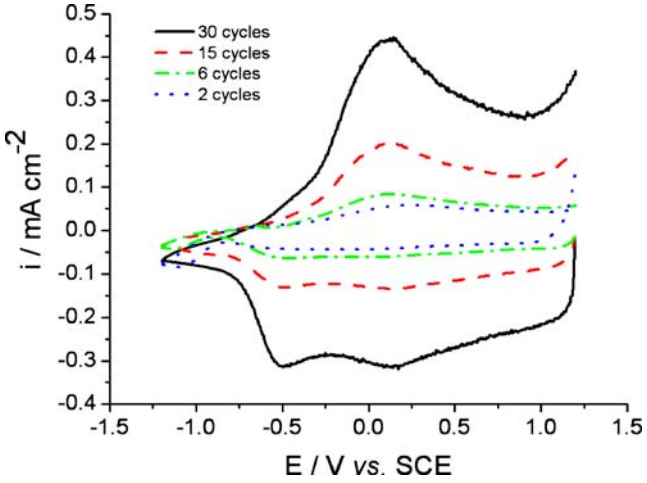

Fig. 5 Cyclic voltammograms of PEDOTh films formed under potentiodynamic conditions with different number of potential cycles, in 0.1 mol dm^{-3} $TBAClO_4$ acetonitrile solution; [−1.2, 1.2] V vs. SCE, υ=50 mV s^{-1}

In order to evaluate and confirm the volume changes accompanying the redox switching of the PEDOTh films, i.e., swelling during oxidation and shrinking upon reduction, a scratch on the modified electrodes have been performed on purpose, in a way to have in the same scanned area bare Pt and polymer film. Figure 8 shows the images and corresponding profiles of the PEDOTh films presented in Fig. 7.

The thickness values indicated in Fig. 8 are a result of several measurements performed for each film; nevertheless, they should be regarded as approximate, since the local roughness of the polymers, induced by the scratch may introduce an error of a few nanometers. Consequently, the data indicates that regardless of the electrochemical polymerisation mode, thin PEDOTh films present similar thickness and swell up ca. 20% upon oxidation. As expected from the analysis of the topographic features exhibited in Fig. 7, the thickness variations were reversible with the potential switching. The obtained change in the PEDOTh thickness conveyed by the redox conversion is in good agreement with that observed in studies concerning other conducting polymers [23, 24].

Taking into account that the polymer thickening is accompanied by the developing of fibber-like clusters (potentiodynamic growth) or of globules of about the same size (potentiostatic growth) differences both in film thickness and in the volume change induced by the redox conversion should be expected in thick films prepared under distinct electrochemical modes. Such work is currently in progress where the authors try to optimize the methodology (for instance *tapping* mode AFM) for the thickness evaluation of oxidised and reduced PEDOTh prepared with at least 30 potential cycles or at constant potential with $Q_g \geq 30$ mC cm^{-2}.

Conclusions

The *ex situ* AFM analysis of PEDOTh films deposited on platinum electrodes under distinct electrochemical modes but displaying similar electroactivity, showed that the layers prepared potentiodynamically present a fibber-like morphology, whereas the ones grown at constant potential exhibit a compact and granular shaped topography. These characteristics provide support to the interpretation of the PEDOTh redox behaviour where, for layers electropolymerised by potential cycling, the polymer reduction appears to occur easier than in films prepared under potentiostatic control.

In situ contact mode AFM provided information on the initial stages of polymer deposition and the surface morphology evolution during the growth of thin layers. Accordingly to that observed *ex situ* for thicker films, the images reveal that polymers grown at constant potential are formed by globules, which diameter increase with the deposition charge whereas, under potentiodynamic control elongated grains develop with the number of polymerisation cycles. For this electropolymerisation mode, the film

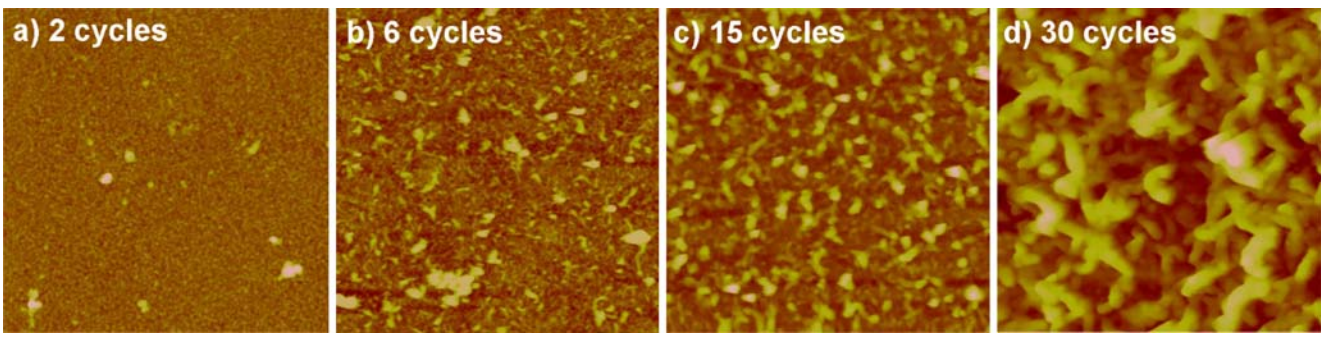

Fig. 6 *Ex situ* AFM-*tapping* mode images (2×2 μm^2) of PEDOTh films potentiodynamically formed with 2, 6, 15, and 30 polymerisation cycles. 2 and 6 cycles: z=60 nm, 15 cycles: z=150 nm and 30 cycles: z=500 nm

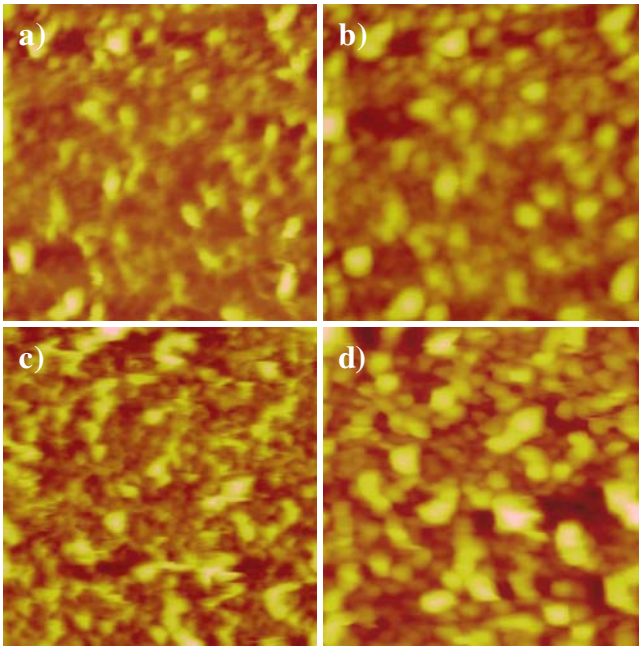

Fig. 7 *In situ* contact mode AFM images (2×2 μm^2) of PEDOTh films in a 0.1 mol dm^{-3} $TBACIO_4$ acetonitrile solution, potentiodynamically formed at 50 mV s^{-1} [−0.8, +1.18] V vs. SCE with 15 cycles in the **a** reduced (at −1.0 V) and **b** oxidised (at 1.0 V) states, z=120 nm; and potentiostatically synthesised (1.2 V, Q_g=21 mC cm^{-2}) **c** reduced (at −1.0 V), and **d** oxidised (at 1.0 V) states, z=120 nm

thickening was further explored by *ex situ tapping* mode AFM and the images unambiguously show that the initial grains evolute into fibber-like aggregates, most notorious after 30 cycles. This type of morphology can be explained by the effect of the ingress and expulsion of counter-ions during each polymerisation cycle, in promoting a structural rearrangement of the polymer which may endorse the formation of longer segments.

The morphological changes imparted by the redox conversion were seen (*in situ* AFM) to be more marked in PEDOTh prepared potentiostatically, which can be attributed to their compact nature, demanding a relatively greater reorganisation during the doping/de-doping processes. Evidence of polymer swelling/shrinking upon redox conversion has been also given by the images acquired for oxidised and reduced films, prepared under both types of electrochemical control. Thickness measurements performed by *ex situ* AFM unveiled that for thin PEDOTh film the volume changes ca. 20% upon oxidation, regardless the method used for the polymer preparation.

The observation of differences imparted by the electropolymerisation mode, certainly better noticed in thicker films, require optimisation of the used procedures, currently in progress.

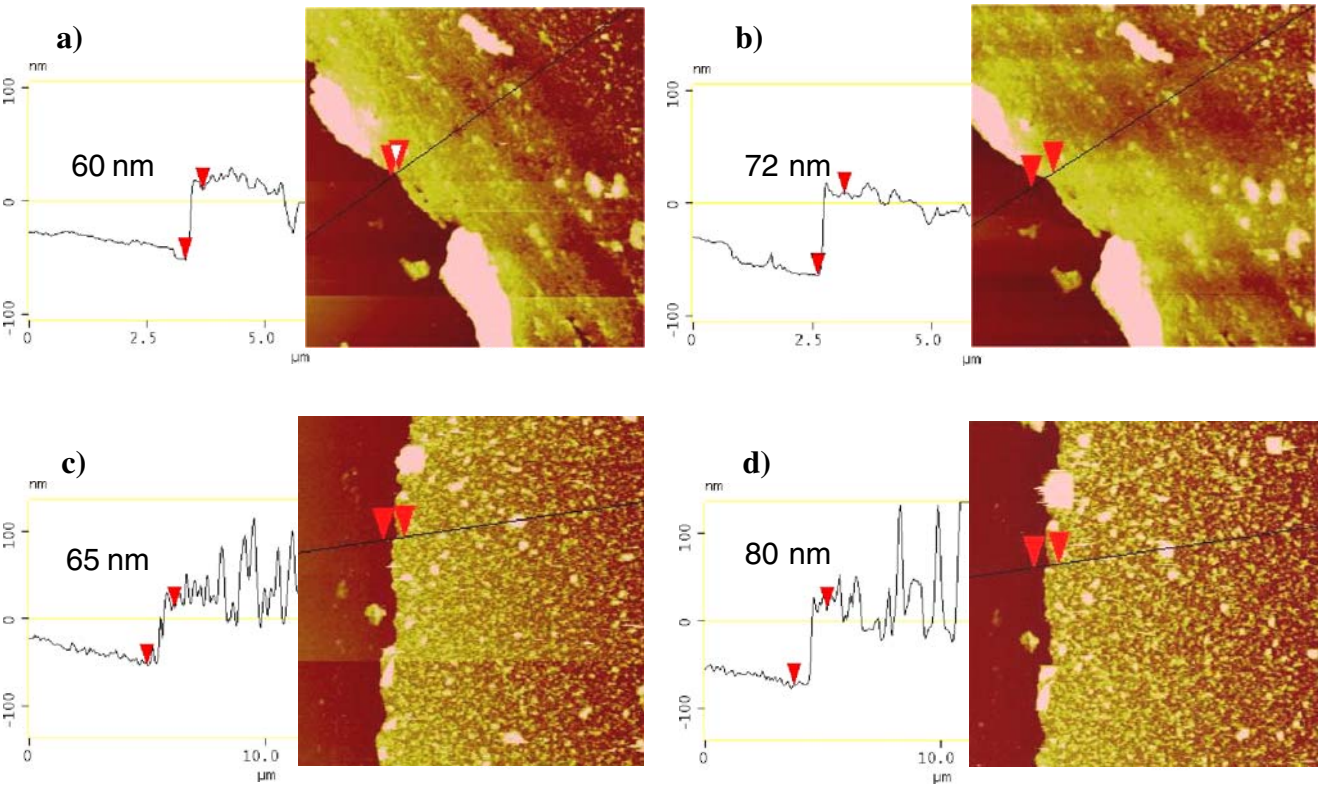

Fig. 8 *In situ* contact mode AFM images of PEDOTh films, in 0.1 mol dm^{-3} $TBACIO_4$ acetonitrile solution, potentiodynamically formed at 50 mV s^{-1} [−0.8, +1.18] V vs. SCE with 15 cycles (10×10 μm^2) at **a** −1 V and **b** 1.0 V; and potentiostatically synthesised at 1.2 V, Q_g=21 mC cm^{-2} (20×20 μm^2) at **c** −1.0 V and **d** 1.0 V; z=210 nm

Acknowledgment A. I. Melato gratefully acknowledges the financial support by "Fundação para a Ciência e Tecnologia" (SFRH/BD/13899/2003).

References

1. Chao F, Costa M, Tian C (1993) Synth Met 53:127 doi:10.1016/0379-6779(93)90885-Z
2. Chao F, Costa M, Jin G, Tian C (1994) Electrochim Acta 39:197 doi:10.1016/0013-4686(94)80055-3
3. Suárez MF, Compton RG (1999) J Electroanal Chem 462:211 doi:10.1016/S0022-0728(98)00414-8
4. Venâncio EC, Costa CAR, Machado SAS, Motheo AJ (2001) Electrochem Commun 3:229 doi:10.1016/S1388-2481(01)00153-9
5. Semenikhin OA, Jiang L, Iyoda T, Hashimoto K, Fujishima A (2000) Synth Met 10:195 doi:10.1016/S0379-6779(99)00283-0
6. Kim Y-T, Yang H, Bard AJ (1991) J Electrochem Soc 138:71 doi:10.1149/1.2085512
7. Mourato A, Viana AS, Correia JP, Siegenthaler H, Abrantes LM (2004) Electrochim Acta 49:2249 doi:10.1016/j.electacta.2004.01.006
8. Innocenti M, Loglio F, Pigani L, Seeber R, Terzi F, Udisti R (2005) Electrochim Acta 50:1497 doi:10.1016/j.electacta.2004.10.034
9. Okamoto H, Kotaka T (1999) Polymer (Guildf) 40:407 doi:10.1016/S0032-3861(98)00248-1
10. Álvarez-Romero GA, Garfias-García E, Ramírez-Silva MT, Galán-Vidal C, Romero-Romo M, Palomar-Pardavé M (2006) Appl Surf Sci 252:5783 doi:10.1016/j.apsusc.2005.07.060
11. Szklarczyk M, Wierzbinski E, Bienkowski K, Strawski M (2005) Electrochim Acta 51:1036 doi:10.1016/j.electacta.2005.05.044
12. Han D-H, Kim J-W, Park S-M (2006) J Phys Chem B 110:14874 doi:10.1021/jp055791b
13. Skompska M, Vorotyntsev MA, Refczynska M, Goux J, Lesniewska E, Boni G, Moise C (2006) Electrochim Acta 51:2108 doi:10.1016/j.electacta.2005.01.066
14. Paczosa-Bator B, Peltonen J, Bobacka J, Lewenstam A (2006) Anal Chim Acta 555:118
15. Patra S, Barai K, Munichandraiah N (2008) Scanning electron microscopy studies of PEDOT prepared by various electrochemical routes. Synth Met. doi:10.1016/j.synthmet.2008.03.002
16. Xiao Y, Li CM, Yu S, Zhou Q, Lee VS, Moochhala SM (2007) Talanta 72:532 doi:10.1016/j.talanta.2006.11.017
17. Melato AI, Viana AS, Abrantes LM (2008) Electrochim Acta (in press)
18. Han D, Yang G, Song J, Niu L, Ivaska A (2007) J Electroanal Chem 602:24–28 doi:10.1016/j.jelechem.2006.11.027
19. Blanchard F, Carré B, Bonhomme F, Biensan P, Pagès H, Lemordant D (2004) J Electroanal Chem 569:203 doi:10.1016/j.jelechem.2004.03.002
20. Du X, Wang Z (2003) Electrochim Acta 48:1713 doi:10.1016/S0013-4686(03)00143-9
21. Niu L, Kvarnström C, Fröberg K, Ivaska A (2001) Synth Met 122:425 doi:10.1016/S0379-6779(00)00562-2
22. Zykwinska A, Domagala W, Lapkowski M (2003) Electrochem Comm 5:603
23. Abrantes LM, Correia JP, Savic M, Jin G (2001) Electrochim Acta 46:3181
24. Barbero C, Kötz R (1994) J Electrochem Soc 141:859